ISSN 0973-3450 (Print)
JUC Vol. 14(4), 126-141 (2018). Periodicity 2-Monthly
ISSN 2319-8036 (Online)

JOURNAL OF ULTRA CHEMISTRY
An International Open Free Access Peer Reviewed Research Journal of Chemical Sciences and Chemical Engineering
website:- www.journalofchemistry.org
Estd. 2005

Molecular interaction mechanism of hydrogen bond disruption of highly viscous glycerol with aniline and derivatives analyzed with physicochemical data

SACHIN B UNDRE[a,c*], SHIVANI R PANDYA[b] and MAN SINGH[c]

[a]Department of Chemistry, Indian Institute of Teacher Education, Gandhinagar 382016, Gujarat (India)
[b]School of Nano Sciences, Central University of Gujarat, Gandhinagar 382030, Gujarat (India)
[c]School of Chemical Sciences, Central University of Gujarat, Gandhinagar 382030, Gujarat (India)
Corresponding Author Email: *sachincug@gmail.com
http://dx.doi.org/10.22147/juc/140402

Acceptance Date 12th March, 2018, Online Publication Date 2nd July, 2018

Abstract

Structural studies of highly viscous liquids are most attracting for several industrial significances. Hydrogen bonding and physicochemical properties (PCP) are critical probe for structural interactions. Thus density ($\rho \pm 10^{-3}$ kg m^{-3}), viscosity ($\eta \pm 10^{-4}$ mPa.S), surface tension ($\gamma \pm 0.01$ mNm^{-1}) and friccohesity ($\sigma \pm 10^{-6}$ sm^{-1}) for aniline (Anl) + glycerol (Grl) [AG], Anl + ethanol (Et) [AE], ortho-Anl + Et [OAE], para-Anl + Et [PAE] binary and Anl + Et + Grl [AEG], o-Anl + Et + Grl [OAEG] and p-Anl + Et + Grl [PAEG] ternary mixtures for entire compositions are reported at 293.15 K. The Anl was soluble in Grl but the OA and PA were not soluble, thereby, the Et was added to solubilize them and noted as interlocutoror hydrogen bond disruptor. The ρ, η,γ andσ were regressed with the Grl mole fractions (x_G) for their ρ^0, η^0, γ^0 and σ^0limiting data with S_ρ, S_η, S_γ and S_σ slope values. The ρ^0as Grl > AEG >AG > PAEG > OAEG inferred stronger interactions with AEG and AG while the weaker with OAEG. The η^0 as AEG >AG > OAEG > PAEG inferred hydrogen bonding (HB) disruption respectively as compared to Grl and decreases the resistance to flow. Their γ^0 as Grl >AEG >AG > OAEG > PAEG weakened 21.60, 33.40, 71.32 and 76.10% cohesive forces (CF) respectively and quantitatively the CF was demonstrated with proposed Spring-Weight (SW) model.

Key words: Interlocutor, interactions, hydrogen bonding, glycerophobic, viscosity, highly viscous liquid.

1. Introduction

Hydrogen bonding (HB) has been in focus for structural characterizations of molecular and molionic mixtures apart from ionic interactions. The HB illustrates a level of PCP for industrial used

materials such as glycerol, honey, corn oil, soya oil and others as they are highly viscous liquids (HVL) with extremely high viscosities from 1490 mPa.S to 2000 mPa.S. Higher viscosity becomes hurdle in designing food products, food supplements and medicine due to weaker mixing activities. The HVL have stronger intermolecular HB whose physiochemical indicators (PCI) such as density[1,2], viscosity, surface tension and friccohesity are authentic data for HB disruption analysis[3]. The PCP of binary and ternary mixtures are highly significant for industrial and research. The AG, AEG, PAEG and OAEG mixtures and physicochemical studies are chosen for HB disruption analysis because these combinations have never been studied and seem to have greater industrial potential in case of multicomponent mixtures. The PCI structurally predicts application suitability for heat and water holding capacities, moderating molecular signals interaction mechanism and responses as well for wider applications in industries. The Grl with 1490 mPa.S is noted as HVL[3,4] with exceptionally stronger intermolecular HB (EXSIHB) which is responsible for weaker solubilizing power of Grl where its 3 free -OH cause EXSIHB with restricted solubilizing activities in medicinal, food products and other formulations. Notably the EXSIHB formation is barrier to mobility and is accurately depicted with physicochemical data where stronger are the HB weaker is the interacting activity. Such liquid mixtures though highly useful but as such no adequate studies are reported in literature as substantial binary and ternary mixtures to be studied for wider database for better choice of their uses. Also the stronger HB structures (HBS) generate a basic vacancy for moderating the EXSIHB to enhance solubilizing capability in formulations and quality control of syrups and others. The EXSIHB could be moderated through chemical additives and thus the Anl along with its o and p derivatives series are chosen for systematic study for molecular modeling for disruption of HB through interacting activities based on mole fractions of the chosen components. Such systems with adequate studies are useful for several industrial applications for saving excess use of Grl. Structurally; the Grl alkyl chain (AC) has covalently bonded 3 C atoms along with highly electronegative 3 O atoms each with 2 unshared electron pairs (USEP) in operational mode for HB. Their USEP caused an internal pressure with stronger Columbic forces which could be weakened with the Et. The AC could weaken due to shared electron pairs (SEP) and stronger covalent bonding force (CBF) which redistribute the molecular forces caused with the USEP. The USEP with Columbic and SEP with the CBF are responsible for EXSIHB as the Anl series interacts with Columbic and CBF with the different PCP. It seems that the OA and PA could not interact directly due to Columbic and CBF where probably the Et facilitated the OA and PA interactions with the Grl. The Et induced additional activities in Grl by disrupting stronger HB with different PCI which acted as excellent sensors in biotechnology, biochemical engineering and biomolecular interactions. The PCP elucidates molecular interaction activities, cohesive forces, frictional forces and surface area of the HVL whose higher values act as an excellent indicator in Grl medium. The study of the PCP of such systems is a challenging task because the Grl acts as a facilitating agent for fluidity and solubility and also the Grl type liquids are not easily mixed with wider chemical substances. Therefore, developing liquid systems for study is restricted and hard-pressed. Though the studies are significant as the Grl with disrupted HB could be attractive to different molecules having electronic, π-conjugation, linear chain, lone pair of electron (LPE) and functional groups. The molecular constituents induce peculiar features to resolve intricacies of interacting activities and draw attention to focus structural alignments. The Et generates or modifies HB based activities but no adequate attention is paid for conceptual framework to generate more database to explore wider uses. Especially, there is an urgent need to explore informatory database on Grl HB activities whose PCP could be significantly moderated for novel industrial uses with efficient mechanism.

Thus the ρ, η, γ and σ as critical PCI studies were chosen and analyzed to ascertain interacting activities of the Anl series on Grl whose intermolecular forces (IMF) are weakened due to Brownian motions (BM)[5]. The BM facilitates an equal distribution of IMF based on Boltzmann distribution to maintain frictional (FF) and cohesive (CF) forces are responsible for medium continuity as an essential condition for σ to

be function of the IMF. The BM rationalizes the σ to be operational and experience a friction due to intensified environment of neighboring molecules with higher surface forces to maintain togetherness due to CF. The FF and CF are highly operative and favor interaction, trapping reorientation, optimization and configuration as the interacting intermolecularfocus understanding of HB conceptually. The HB monitors behavior of mixtures and thus many parameters were studied together for a complete interaction scenario.

The Grl is a remarkable solvent for organic and inorganic substances with stronger HB and excellent solvent activity for effective intermolecular activity (IMA). The IMA induces plasticizing action on proteins and gelatine to tolerate a larger Grl amount and still remain a firm gel, which is not with glycols or glycol ethers. Equation 1 depicts induced polarizability (α) in such organic molecules with mild electrostatic forces (ESF) and the α on a pattern of ionization explain the interactions[6].

$$E^{disp}{}_{AB} \approx \frac{3\alpha^{A}\alpha^{B}I_{A}I_{B}}{4(I_{A}+I_{B})}R^{-6} \qquad (1)$$

The dispersion energy E^{disp} between A and B molecules caused induction I_A and I_B at distance R. The mixtures are thermodynamically active and utilize energies with a net force with $\Delta G \neq 0$ and explained with equation 2.

$$F_{nimf} = F_{Glr} - F_{Anl} = \frac{1}{4\pi\varepsilon_0}\left[\frac{q_{Grl}^{-}q_{Anl}^{+}}{r_{Grl}^{2}} - \frac{q_{Grl}^{-}q_{Anl}^{+}}{r_{Anl}^{2}}\right] \qquad (2)$$

The F_{nimf} is net IMF, F_{Grl}, F_{Anl} are forces associated with Grl and Anl, q_{Grl}^{-} and q_{Anl}^{+} electrostatic poles responsible for interacting activity for molecular interaction dynamics (MID). For example, equations 1 and 2 trap a net force as $F_{Grl} \neq F_{Anl}$ as the activities of both the phases are unequal and polarization caused spontaneity. Though the mixtures are away from ideal gas behavior as IMF ≠ 0 and shear stress and strains exist in dissimilar molecules. It inferred interacting dynamics with reorientational motions with molecules such as Grl. Thus our study could be useful for such activities.

2. Experimental and Methodology :

The Grl, Anl, OA, PA and Et (AR, 99.99%, Ranbaxy, India), were used as received. The OA and PA were insoluble in Grl and were separately dissolved in Et in 0.1:1.19 ratios, w/w as binary stock solutions of Anl, OA and PA which were separately mixed with Grl in 1: 5 ratios, w/w. The Anl and Grl mixture prepared in 1: 5 ratios and were studied for a role of Et as an interlocutor. The ρ was measured with Anton paar Density and Sound velocity Meter (DSA 5000 M) by filling 3 mL in DSA Quartz U tube within 20 sec as filling time. Before each samples of measurements, the instrument was calibrated at atmospheric pressure with Millipore water and dry air. For η, γ and σ data, the pdn and t were measured with Borosil Mansingh Survismeter[7-10]. The Survismeter was properly cleaned, dried and vertically mounted at 90 degree angle in thermostat of ± 0.05^0 C. For each sample, several measurements were conducted. The calibration was made with Millipore water whose 10 to 15 measurements were repeated to ensure reproducibility in data. Adequate statistical data analysis made attempted to calculate standard deviation and confidence variance. The 95.5% confidence variance was found in the data. The procedural details of experimental methods with survismeter are reported elsewhere[9-11]. It worked based on carburetor and bypassing concepts incorporating R_4 (Reduce, Reuse, Recycle, Redesign) M_4 (Multipurpose, Multidimensional, Multitasking, Multifaceted) for resources and time saving by 98% as compared to usual.

2.1 Contact angle theta (θ) correction :

Conceptually the cohesive force generated surface tension and the liquid mixtures when were allowed to flow within capillary of fixed id (r, mm) the liquid gets accumulated at circumference and formed pdn around outer surface of the capillary. The weight (mg) of individual drop formed at a lower circumference of a capillary of specific id becomes equal to surface tension (γ, mN/m). It is depicted as in equation 3.

$$mg = \pi r\gamma \ Sin\ \theta \qquad (3)$$

The m is mass of an individual drop, g gravitational force (9.81 ms^{-2}), r capillary id, and the θ is contact angle in degree. In general, a falling pdn around a capillary circumference forms a contact angle $\theta < 90^0$. The tip of a capillary was sharpened and formed a contact angle $\theta = 90^0$ where Sin 90 =1. The sin 90 =1 is

kept in equation 3 depicted as equation 4.

$$mg = \pi r\gamma \quad (4)$$

It was a basis for pdn determination and use for surface tension and interfacial tensions calculation in air and liquid mixture with their fixed buoyancies.

3. Results

The ρdata are given in table 1 and the ρ inferred internal pressure due to IMF that influenced oscillation periods of quartz tube. A higher internal pressure reduced volume V_2 as $PV_2 = K$, a Boyle's law where a higher internal pressure produced a lower V_2 and higher densities as in equation 5.

$$\rho = m/V \quad (5)$$

The ρ and ρ_0 are solution and solvent densities respectively, m molality, M is molar mass respectively. The t and n data calculated friccohesity with Mansingh Equation 6.

$$\sigma = \sigma_0[(t/t_o \pm B/t)((n/n_o) + 0.0012(1-\rho))] \quad (6)$$

The σ_0 is glycerol friccohesity derived from η_g/γ_g (η_g = viscosity, γ_g = surface tension) and noted as baseline for interactions reported elsewhere[10]. B/t, a kinetic energy correction, $0.0012x10^3$kg m^3 air density and (1-ρ) is buoyancy correction. The B/t and Survismeter constant (K_{vis}) were derived from $\eta=\rho(K_{vis}-B/t)$. The B/t and 0.0012(1-ρ) are $0.18x10^{-6}$ and $1.89x10^{-6}$ at 298.15 K, respectively. The K_{vis} with Milli-Q water was calculated with $\eta/\rho = Bt-V/8\pi$ r Lt and the V is volume that flows, r radius and L is capillary length[11, 12]. The equation 3 becomes 4 on omitting B/t and buoyancy correction values.

$$\sigma = Mc\ (t.n) \quad (7)$$

The $Mc = \sigma_0/(t_0n_0)$, a Mansingh constant[11]. The K_{vis} was calculated with equation 8.

$$\eta = K_{vis}\ \rho\ t \quad (8)$$

The symbols are as usual and the η was calculated with equation 9.

$$\eta = \eta_0(t/t_0)\ (\rho/\rho_0) \quad (9)$$

The K_{sur} Survismeter constant for surface tension unit was calculated with equation 10.

$$\gamma = K_{sur}\rho/n \quad (10)$$

The K_{sur} was used for surface tension calculation with equation 11.

$$\gamma = (n_0/n)(\rho/\rho_0)\gamma_0 \quad (11)$$

The η, γ and σ data for the Grl, Anl, GE,AE, OAE, PAE, Et and water measured individually, are given in table 1 and their mixtures in table 2. The regression constants are given in table 3a and 3b.

4. Discussion

Electronegativity developed the ESF for the HB interaction[13] due to a shift of covalent electron pair (CEP) towards a high more electronegative atom that disrupted Grl HBS and Anl HBS (Fig. 1a and 1b). The Linus Pauling described [14] interaction due to electronegativities as in equation 12.

$$\chi_A - \chi_B = \frac{1}{eV^{1/2}}\sqrt{E_d(AB) - \left[\frac{E_d(AA)+E_d(BB)}{2}\right]} \quad (12)$$

The E_d is dissociation energy, the χ_A and χ_B are electronegativities of A-B, and A-A and B-B type of molecules which facilitated the mixing with increase rise in temperature. Individually, the Grl is soluble with Anl and the Et with Anl, OA, PA and Grl for binary systems their PCI given in table 1 and interacting models are in figs. 1 and 2. (Table 1 and Figs. 1c, 1d).The OA and PA did not facilitate interact with Grl despite being a chemically active with high potential interacting capability. The Et act as a moderator to enhancing interacting activities of interacted with Anl, OA and PA with Grl as ternary systems for a favorable environment to dissolve OA and PA in Grl due to partially HB disruption partly. The ESF is responsible for interactions which are explained with Lennard-Jones potential [6] depicted in equation 13.

$$\upsilon = 4\varepsilon\left[\left(\frac{\sigma}{r}\right)^{12} - \left(\frac{\sigma}{r}\right)^{6}\right] \quad (13)$$

The ε is a minimum potential depth, σ is intermolecular distance and r is separation of ESF and CBF. A charge separation of among individual molecules showed a comparable variation in HB disruptions (Tables 1and 2). The ESF induced dipole-dipole (d-d) and dipole-induced dipole (d-d_i) interactions and emerged out of molecular asymmetric geometry with positively induced electrostatic energy

(+ve IE) with electrostatic centers encountered as and depicted in equation 14.

$$IMF_{Grl\text{-}Anl} = - \frac{\vec{\mu}_1 \vec{\mu}_2}{4 \pi \varepsilon r^6} \qquad (14)$$

The $\vec{\mu}_1$ and $\vec{\mu}_2$ are vector potentials of the ESF, both theand r are as usual where the charge accumulation of electronegative O atom of the Et could induces interacting force to interact with solubilize in Grl. The IMF induces kinetic state with viable energy for interactions or HB disruptions. The OAE and PAE structures interacted with Grl structure where the -NH_2 at o and p positions weakened interacting activities of the Anl-NH_2 with disruption and release of a lone pair electron (LPE). The Figs. 1e and 1f depict OAE and PAE structures along with Grl where the -NH_2 at o and p positions weakened interacting activities of the Anl-NH_2 with disruption and release of a lone electron pair (LEP). The Et enhanced OA and PA interacting activities with solubility in the Grl. The 2.7, 1.59 and 1.69 Debye dipole moments of Grl, Anl and Et are respectively also responsible for interactions. The AE, OAE and PAE with Grl as ternary systems have lowered the densities as compared to the Grl and behaved as structure breakers with comparatively weaker IMF. The Grl with highly electronegative 3 O has developed stronger ESF in binary as well as ternary mixtures. The Grl and Et worked with electronegativities and caused Columbic forces and vander Waals forces while the Anl worked on the π- conjugation interaction with higher IMF response to of the Grl and Et while OA the weaker. The lone pair electron of -NH_2 is repelled out by that of another -NH_2 at o-position due to a close proximity that created a steric hindrance causing stronger activities than of the PA and also but the weaker than of the Anl as is explained with equation 14. However, a repelling force with PA is weaker due to a larger distance between 2-NH_2 them in comparison to OA but both the OA and PA as glycerophobic were not directly interacted dissolved with Grl and the Et initiate interaction between them with Grl. dissolved. Such structural interactions of the Et have decreased theρ, η, and γ by 35.24, 38.27, 7.08, 99.89 and 63.48 % as compared to Grl (Table1). The Anl and Et both behaved as structure breakers and the Et with maximum decrease with Anl caused stronger structure breaking action (Table1). The mixtures with $\eta_{sp} = (\eta\text{-}\eta_0)/\eta_0 = (\eta_r\text{-}1)$, the $\eta = \eta_0$ with $\eta_{sp}=((\eta/\eta)\text{-}(\eta/\eta))$ or $\eta_{sp} = ((1)\text{-}(1))$ or $\eta_{sp} = 0$ infer an ideal state with non-interacting activities and noted as IMF = 0 but the Grl showed $\eta > 0$. The IMF > 0 inferred stronger interacting activities. The Grl mixtures showed with $\eta_r = 1 + B\,m$, the $B = \Delta y/\Delta x$. The $1 = 1 + B\,m$, if the $B\,m = 0$ then the $\Delta y/\Delta x = 0$ but the $\Delta y/\Delta x \neq 0$ and the $\eta \neq \eta_0$ or $\Delta y/\Delta x \neq 0$ and inferred interacting activities[10, 12].

4.1 Density :

The density predicts a level of IMF where the Grl with 1.258271 kg/m^{3}at 20^{0}C has stronger IMF with stronger CBF as shared electrons are confined in shared orbital and highly electronegative O with lone pair of electron[15]. Comparatively, the Grl density is 1.26 times higher than of the H_2O with 1.26 times higher IMF due to stronger HB with 3-OH and CBF and due to USEP with Grl and Vander Waals forces with water (Table 1). The latter has caused stronger Columbic force with exceptionally higher internal pressure with higher density and viscosity[11, 12]. The table 1 found densities as Grl > Anl >PAE > OAE > AE > Et inferred stronger HB and higher IMF with Grl, Anl and also weaker HB and lower IMF with the PAE, OAE, AE and Et. due to with higher values of the Grl and the Anl due to stronger HB and stronger higher IMF than of the OA, PA and Et with the weaker HB and weaker IMF also a delocalized structure of the Anl structure (Fig. 1g). The Anl, OAE and PAE densities are lower than of the Grl due to weaker IMF with Anl, OAE and PAE than of the latter (Table 1). The Anl derivatives and Et in Grl with lower densities and weaker IMF with HB disruption behaved as structure breakers. Lower density of Grl infers weaker internal pressure with structures breaking effect of the Anl derivatives and Et on Grl structure. For example, the -NH_2 with the Anl developed a stronger IMF and the Et has weakened due to HB disruption where in binary systems the Et also behaved as structure breaker. The table 1 depicted comparatively higher densities with ternary systems than of the binary by 0.44627 % due to stronger HB.

The Grl with Anl decreased densities with weaker IMF due to weaker HB and also π-conjugation effect of the Anl[1]. The Grl density is 1.23 times higher than of the Anl with 1.23 times weaker IMF (Table 1). The ρ^0 as AEG > AG > PAEG > OAEG elucidated stronger interactions with AEG and AG due to stronger HB and π-conjugation in Anl interacting HB models with stronger IMF and higher IMA due to -NH_2 and -OH while the weaker with OAEG (Table 3a and Figs. 1c, 1d). The Grl with 3-OH caused a stronger HB as its each H is bonded with 3 Anl molecules with stronger HB. The Anl has highly stronger π-conjugation with higher ρ^0 (Fig. 1c). The Et with the OAEG and PAEG as interlocutor induced weaker HB than of the AEG (Fig.1d). The PAEG has symmetric and OAEG asymmetric structures without any π-conjugation due to two donating -NH_2 and the Et weakened the HB (Figs. 1e, 1f). The equations 1 and 2 explained the interaction vacancies where the pi-conjugation caused charge accumulation sites. The higher ρ^0 of the PAEG than of the OAEG inferred stronger activities (Table 3a). With OAEG the -NH_2 is at o and with the PAEG at p-positions induced the interactions but their π bonds, it does not form π-conjugation. Thus at o and p positions electronic interactions are absent with the weaker IMF of the OAEG than that of PAEG respectively. Similarly, the AG, AEG, OAEG and PAEG have no electron exchange without any correlation with electrophile and nucleophile. Though the partially electrophile and nucleophile interactions with AG, AEG, OAEG and PAEG could be considered as their ρ is increased (Table 2). It inferred that the interactions associated with Anl dissolution with Grl due to π-conjugation are with stronger HB (Fig. 1c). With the OAEG and PAEG without π conjugation with weaker HB than of the AG showed the ρ^0 as AEG >AG> PAEG > OAEG (Tables 3a, 3b). It inferred that the Et developed stronger HB with both the AEG and AG monitor the HVL as the with density increases with increased x_G (Table 1).

4.2 Surface tension :

The γ of Anl, AE, OAE and PAE are lower than of the Grl as the $\gamma(Nm^{-1})$ or surface energy (Jm^{-2}) is caused with stronger CF within the similar molecules (Table 1). The IMF is directly proportional to the CF hence, Thus the stronger is IMF higher is the CF [11, 12]. The AE, OAE and PAE weakened the Grl IMF due to AEG, OAEG and PAEG interactions with comparatively weaker IMF in ternary mixtures as compare to AG, OAG and PAG binary mixtures. The weakening of the CF inferred that the weaker IMF is caused due to SEP that caused interactions with -NH_2 numbers and its positions. The Et with -OH disrupted the HB network (HBN) of the Grl. Comparatively, the PA due to symmetric -NH_2 placement substantially weakened the CF. However from 0.35 to 0.55 x_G the γof PAEG is slightly higher than of the OAEG and from 0.65 to 0.90 x_G the lower (Table 2). The PAEG concluded that the surface activities due to -NH_2 positionare influenced by the concentration. The γ values with 0.48 x_G increased from 22.5 to 38 mN/m and a further decrease to 32 mN/m inferred surface activities (Table 2) of the PAEG. The γ^0 as AEG> AG > Et inferred the Et act as interlocutor as it has strengthened the AEG interaction activities. However the Et has developed the HB with H of the Anl with lower values of the γ^0 than of the AEG (Table 1, 3a and Fig. 1d). The Et weakened IMF of the Grl but strengthened that of the AEG as the AG has produced γ from 43 to46 mN/m within range 0.55 to 0.92 x_G with a slight variation in conc. with weaker effect on CF (Table 2). It may be due to stronger HB whose activities are concentration independent. With these effects the structural interacting model depicted in fig. 1c inferred several sites to develop intensive HBN with AG, it depicted a state functions with maximum values of the PCI than of the others except Grl (Tables 1 and 2). The Et intensified the HB with stronger IMF depicted with higher PCI values directly proportional to structure networking through HB in AEG (Fig. 1d). The Fig. 1h proposed a Spring-Weight (SW) model has analyzed a decrease in downwards pull and proposed a Spring-Weight (SW) model showing the cohesivity and, it supported with higher γ^0 of the Grl with stronger IMF and higher CF noted as AEG> AG > OAEG > PAEG with 2.79: 3.28: 1: 4.90 ratios with lower γ^0 due to weaker IMF and lower CF with the PAEG (Table 3a, Fig. 2). The disrupted π-conjugation of OAEG and PAEG with infinite Grl dilution has produced a lowest value of the γ^0. The Grl with OAEG and PAEG with minimum Grl conc. act as least energy

surface liquid with exceptionally least γ^0 values (Table 3a) also Et enhancing the surface activity with OAG and PAG. Comparing the γ data of table 2 inferred that the AE, OAE and PAE showed higher than their mixtures with Grl (Table 1and 2). The Grl has seriously weakened the CF of AE, OAE and PAE may be because of due to disrupted π-conjugation that disrupts the disrupted Grl HB in case of with AEG. An proposed interlocutor model applied with the OAEG and PAEG has reduced the CF and IMF for better application (Figs. 1e and 1f). Likewise similarly the S as PAEG > OAEG > AG >AEG with 46.43, 29.65, 9.47 and -37.38 mN kg $mol^{-1}m^{-1}$ has inferred strongest CF with weakest PAEG and AEG weakest composition effects respectively on the surface tension scale (Table 3a and Fig. 4). The slope values revealed a higher Grl response to the PAEG by getting fitted with PA and Et with stronger IMF. Similarly, the Grl composition strengthened its acceptability due to its utilization with the PA and Et interactions. The Sγ> 0 data inferred the PA and Et interactions with Grl and increment in x_G enhanced the interacting activities of the PAEG (Table 2 and 3a). The Et has reduced the AG interactions by -3.95 times by disrupting AG structure that developed weakest bonds with both of them (Table 3a). Thus, the Anl π-conjugation though is effective with AG but with the Et the activities are weakened. Separately, the Grl, Anl and Et with large number of USEP and excess electron density neither of them is able to induce stronger interactions as LPE of Anl not acceptable by either Grl or Et due to repulsive forces. With increase in composition the weaker IMF is developed with weaker CF but with one more $-NH_2$ at p position and PAEG with Grl showed 4.9 times conc. effect with strongest action (Tables 2 and 3a). Hence Therefore, the 1-NH_2 enhanced interacting capability of the Grl. And similarly when the $-NH_2$ is placed on o position then conc. effect is weakened as compared to $-NH_2$ at p position.

The OAEG in comparison to AEG showed 3.13 times interactions due to interacting influence of additional $-NH_2$ (Table 3a). The OAEG and PAEG study confirmed that the disrupting π-conjugation enhanced interacting activities with Grl compositions as compared to the AEG. Probably the AEG with negative slope and with increment in Grl conc. inferred a movement towards interface with maximum surface energy utilization resulting into a lower γinferred weaker CF (Table 3a). The negative slope also inferred stronger activities at air-liquid interface (ALI) with increase in Grl conc. and a continuous accumulation decreased surface energy. The SW showed an elevation in downward pull due to weaker tension at ALI with competitively weaker activities in bulk phase (Fig. 1h). The surface tension and viscosity go hand in hand with an excellent science of molecular activities and interaction. A positive slope showed a maximum molecular accumulated in bulk phase than of the ALI with stronger forces but surface excess concentration of AE decreased γ values. Thus the two forces worked together where one with a stronger down word pull due to stronger IMF while another weaker IMF and stronger CF or surface activities. The slopes defined molecular activities with composition visa-e-vise stronger or weaker IMF with respectively. The γ and η data showed similar trends with Et due to weaker A-HB-G transforming into further weaker E-A-HB-G-A-E network via HB with weaker IMF as compared to the Grl. Thus the Et has moderated a mixture of lower γ and η with higher spreading capacity as PCI. For example, The Et has reduced γ by 50% and the η by 300 from Grl to AG the Et with AG by bringing a HVL Grl to moderately viscous. The Anl has reduced the η of the Grl by 33.58% whereas the Et has reduced η of the AG by 40% (Table 2). Comparatively the PA and OA reduced the γ of the Grl with Et by 23.42 and 23.99, respectively (Table 1). Here, the PCI behaved as critical sensors for deciding a fate of industrial processes.

4.3 Viscosity and Friccohesity :

The IMF is directly proportional to the HB and applicable to viscous flow as an essential condition for viscosities. For example, a higher ηof the Grl is due to stronger EXSIHB than of the Anl, OA and PA. The η as Grl > Anl > OAE > PAE > AE > Et noted weaker IMF with $-NH_2$ at O and P positions in OA and PA as compared to the Anl (Table 1). Though the IMF was stronger than those of the AE due to higher interacting activities of the $-NH_2$ than of the $-NH_2$ of Anl with Et and hence the $-NH_2$ position with numbers influenced the activities. The η as Grl >

mixture has inferred HB disruption of Grl with Anl, AE, OAE and PAE weaker interactions that also analyzed a binding capability of Anl derivatives with Grl (Tables 1, 2). The η^0 as AEG >AG >OAEG >PAEG as compared to Grl inferred stronger structural interaction of the AG than that of PAEG (Table 3b, Fig 5). The Et weakened IMF of AG with comparatively weaker FF than of AEG. Further the $-NH_2$ at o and p positions with GE weakened the FF. Comparatively the $-NH_2$ at o-position caused a higher FF than that of the p-position whose geometry supported structural models (Figs. 1e, 1f). The PAEG has symmetric and OAEG asymmetric structural geometries with weaker and higher activities respectively. Thus either the $-NH_2$ of the Anl or of the OA and PA monitor structural interactions and the Et interaction is noted as complementary to the $-NH_2$ activities. The positional activities increased the ρ and σ with increase in x_G depicted in table 2 with stronger IMF with higher activities[10, 13]. The interacting sites in Anl, OA and PA are strongly tied-up with Grl and assisted with the Et via HB (Figs.1d, 1e and 1f). The interacting series of Anl undergo activation and geometrical changes with stronger interaction forces. The HBN of the Grl is responsible for Columbic interaction with Anl, AE, OAE and PAE. The Grl HBN where the 3-OH and AC as backbone developed stronger HB structure while the Anl has disrupted the HB with another HBN (Figs. 1a, 1c). Interestingly the η and σ have similar trends with different data with x:y ratios (Table 2). The σ^0 value is near to fundamental and molecular constitution based important properties property. Conclusively the σ^0 as AEG > AG > PAEG > OAEG supported a trend of ρ^0 with stronger friccohesive forces (Figs. 2, 3). The η conceptually explained a structural mechanism to moderate a fluid dynamics while the σ [8,9] completely elucidate a probably distribution, unification, diversification, accumulation and operational forces with FF and CF together. The σ is highly relevant data of fluid dynamics and illustrates rheological behavior through structural reorientations and alignment of IMF in the molecules. The data in table 2 and figs. 3, 5 explained a relationship of FF with CF for surface and bulk phase activities respectively. For example, the CF directly depicts molecular electronics due to dipole moment and analysis of FF phenomenon during fluid flowing and not in static condition.

Of course, ESF monitored the FF but still it is not so effective while the σ is studied to derive new scientific simulation of controlling forces in measurements. The CF is incorporated in determination for the σ where a practical situation is that a fluid flows within fixed boundaries where the FF becomes operational in continuum model. The FF has inverse relation with CF and is operational and responsible to maintain continuous flow (Table 2 figs. 3, 5). On flow, the molecules are not separated like gases which are applicable in flow of single molecular, bimolecular and trimolecular liquids**.** Interacting mechanism is depicted and reflected through HBN (Figs. 1a-1f). The -OH and 2 $-NH_2$ have produced higher density of USEP and resistedto HB possiblity. Both the O and N atoms are more electronegative with stronger Coulomibc forces. The Grl with exceptionally stronger IMF has showed a higher viscosity of 1490 mPa.S and the Anl, AE, OAE and PAE has decreased by 99.75 , 98.87, 99.60 and 99.73%Anl has decreased the same by 99.75, AE by

Table 1. Physicochemical data of Grl, Anl, GE,AE, OAE, PAE, Et and water.

Pure system	ρ	η	γ
Glycerol	1.258271	1490	64.00
Aniline	1.021654	3.7100	42.70
GE	0.814834	1.5859	23.37
AE	0.810900	1.2667	25.68
OAE	0.816528	1.7886	23.42
PAE	0.828500	1.8149	23.99
Ethanol	0.791948	1.2000	22.39
Water	0.998196	1.0020	72.88

Table 2. Mole fractions ($x \pm 10^{-4}$), densities ($\rho \pm 10^{-3}$ kg m^{-3}), viscosity ($\eta \pm 10^{-2}$ mPa.s), surface tension ($\gamma \pm 10^{-3}$ mNm^{-1}), friccohesity ($\sigma \pm 10^{-2}$ sm^{-1}) at 20°C.

AG				
x_G	ρ	η	γ	σ
0.9181	1.257170	660.14	43.906	15.04
0.8329	1.217024	369.70	43.507	8.50
0.7441	1.186264	271.72	45.177	6.01
0.6515	1.165600	239.77	45.301	5.29
0.5548	1.139930	138.65	46.199	3.00
0.4538	1.117648	128.41	44.347	2.90
0.3482	1.093958	132.84	44.100	3.01
0.2376	1.070488	135.58	44.333	3.06
0.1216	1.045473	138.67	44.018	3.15
AEG				
0.8460	1.215262	417.22	42.37	21.05
0.4467	1.048751	33.73	39.07	1.85
0.3499	1.019907	23.14	41.33	1.20
0.2570	0.948289	0.96	38.08	0.025
0.1679	0.904439	0.51	38.98	0.013
0.0823	0.857124	0.24	39.64	0.006
OAEG				
0.8789	1.224675	457.96	54.658	17.91
0.7633	1.183475	296.91	46.526	13.64
0.6529	1.140834	109.56	41.991	5.58
0.5473	1.096262	54.66	39.255	2.98
0.4463	1.050251	30.67	38.503	1.70
0.3495	1.006158	13.93	42.252	0.70
0.2568	0.955858	0.45	23.787	0.02
0.1677	0.907707	0.25	23.725	0.01
0.0822	0.864843	0.15	23.654	0.01
PAEG				
0.8773	1.218771	419.45	52.128	17.17
0.7606	1.183285	242.69	43.380	11.93
0.6496	1.136804	98.14	41.348	5.06
0.5437	1.094446	59.42	39.343	3.22
0.4427	1.048180	21.05	39.525	1.14
0.3462	1.028824	15.76	43.697	0.74
0.2540	0.995624	8.36	23.518	0.35
0.1657	0.960227	5.89	23.305	0.25
0.0811	0.880005	2.97	22.665	0.13

Table 3a. Regression constant ρ^0 (kg m^{-3}), $S\rho$ ($kg^2\ m^{-3} mol^{-1}$), $S\rho^1$ ($kg^2\ m^{-3} mol^{-2}$) and γ^0 (mNm^{-1}) $S\gamma$ ($mN\ kg\ mol^{-1} m^{-1}$) $S\gamma^1$ ($mN\ kg^2 mol^{-2} m^{-1}$).

System	Density			Surface Tension		
	ρ^0	$S\rho$	$S\rho^1$	γ^0	$S\gamma$	$S\gamma^1$
AG	1.0316	0.1284	0.1194	42.62	9.47	-8.92
AEG	1.0619	0.9881	1.2309	50.16	-37.38	30.98
OAEG	0.8139	0.3919	0.0619	18.35	29.65	7.77
PAEG	0.8534	0.3599	0.0358	15.29	46.43	-10.69

Table 3b. Regression constant σ^0 (sm^{-1}), $S\sigma$ (sm^{-1} Kg mol^{-1}), $S\sigma^1$ (sm^{-1} $Kg^2 mol^{-2}$) and η^0 (Kg m^{-1}), $S\eta$ ($Kg^2 mol^{-2}$), $S\eta^1$ ($Kg^3 mol^{-3}$).

System	Viscosity			Friccohesity		
	η^0	$S\eta$	$S\eta^1$	σ^0	$S\sigma$	$S\sigma^1$
AG	289.67	-1106.93	1549.69	6.728	-26.103	36.117
AEG	1431.16	-4912.16	4061.31	72.007	-247.35	204.68
OAEG	135.64	-977.20	1395.65	4.658	-34.995	53.023
PAEG	128.30	-883.91	1247.14	4.774	-33.949	50.324

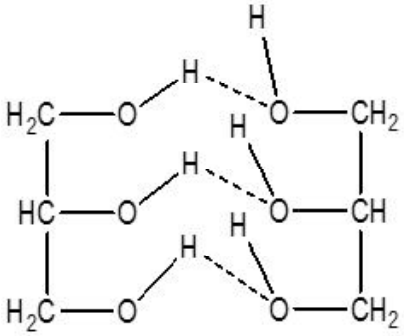

Fig. 1a : Glycerol interacting HB in pure form.

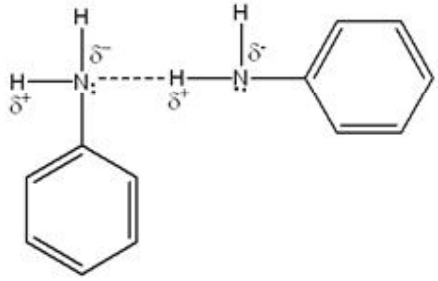

Fig. 1b : Aniline interacting HB in pure form.

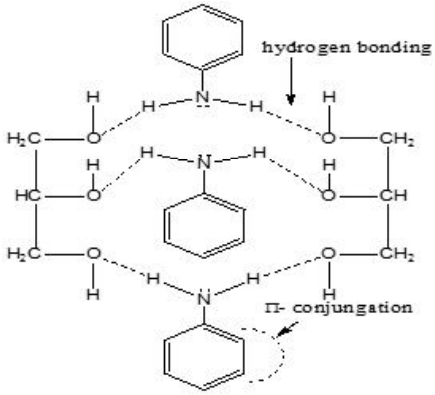

Fig. 1c : AG intracting HB model.

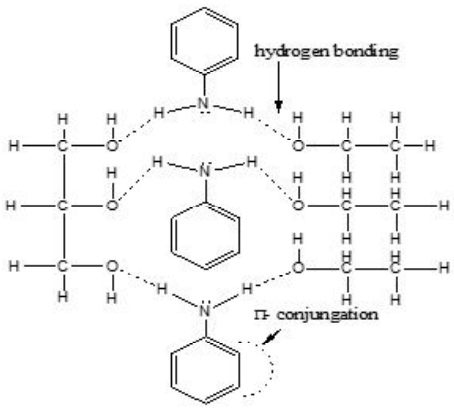

Fig. 1d: AEG interacting HB model.

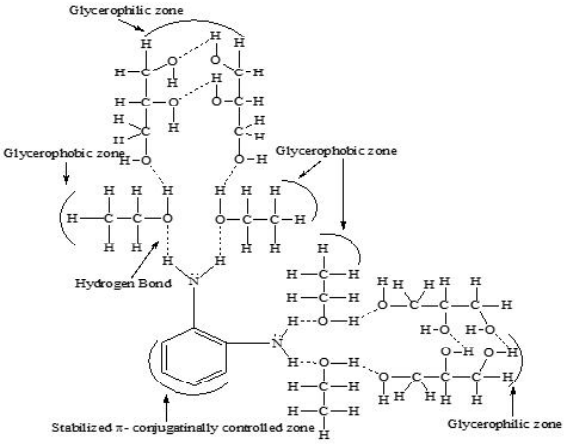

Fig. 1e. OAEG interacting model accelerated with ethanol as interlocutor.

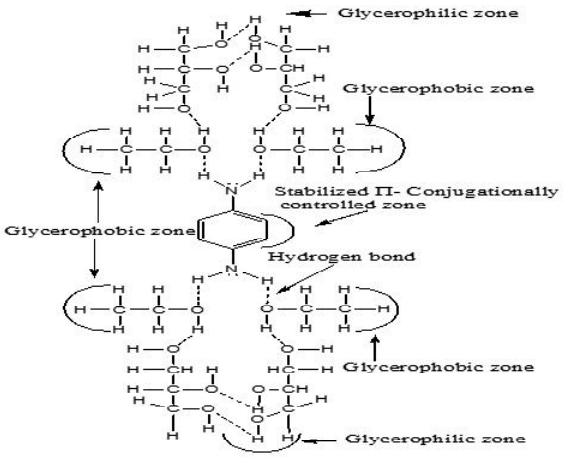

Fig. 1f. PAEG interacting model accelerated with ethanol as interlocutor.

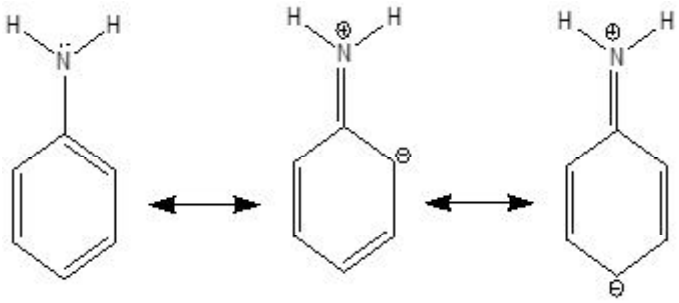

Fig. 1g. Resonance forms of aniline.

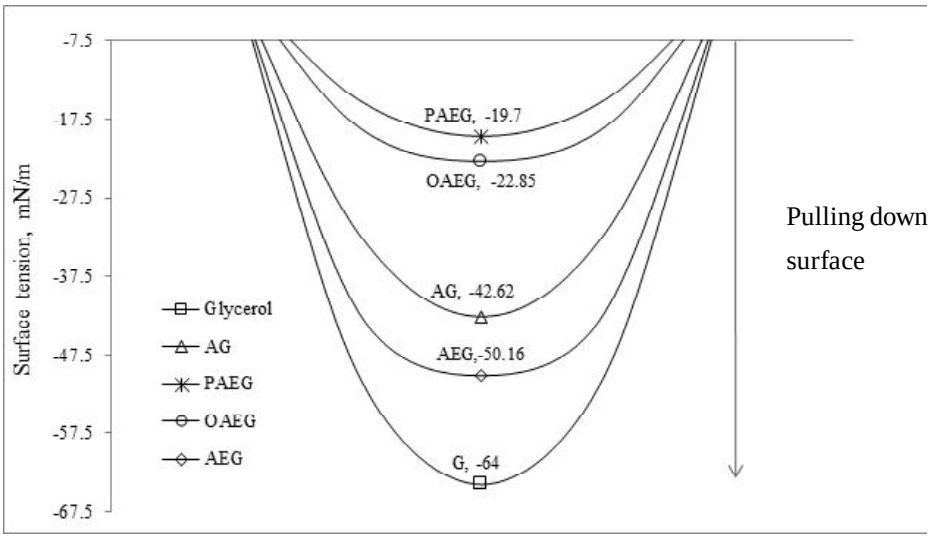

Fig. 1h. Spring-weight surface energy consumption model supported by γ data.

Fig. 4

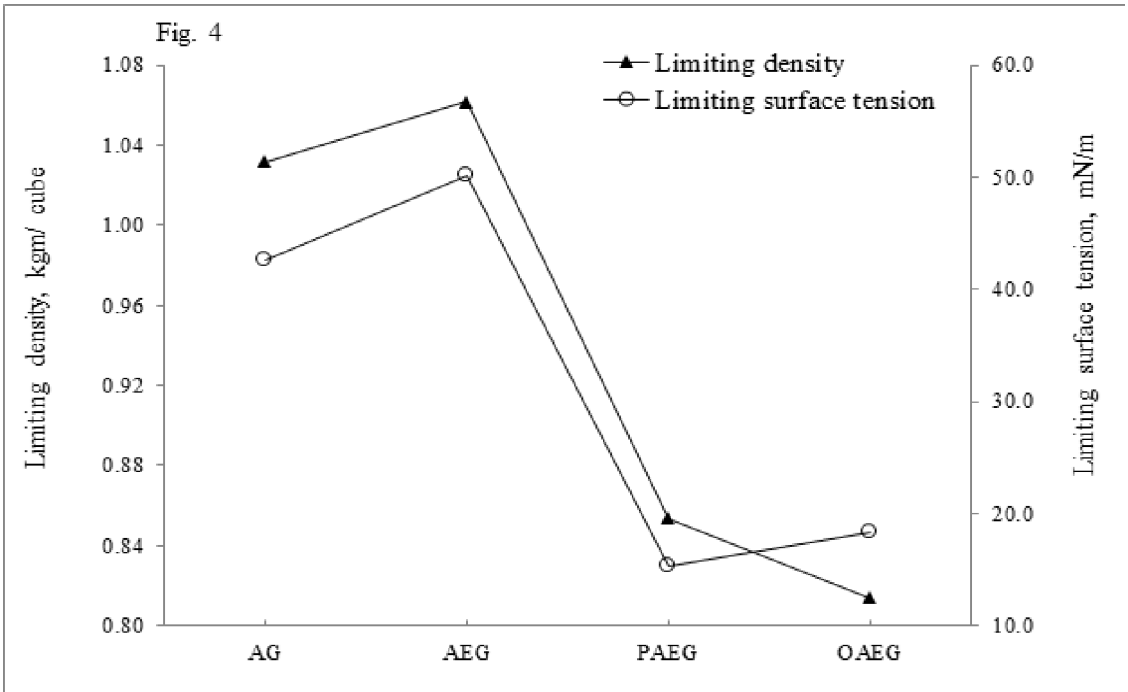

Fig. 5

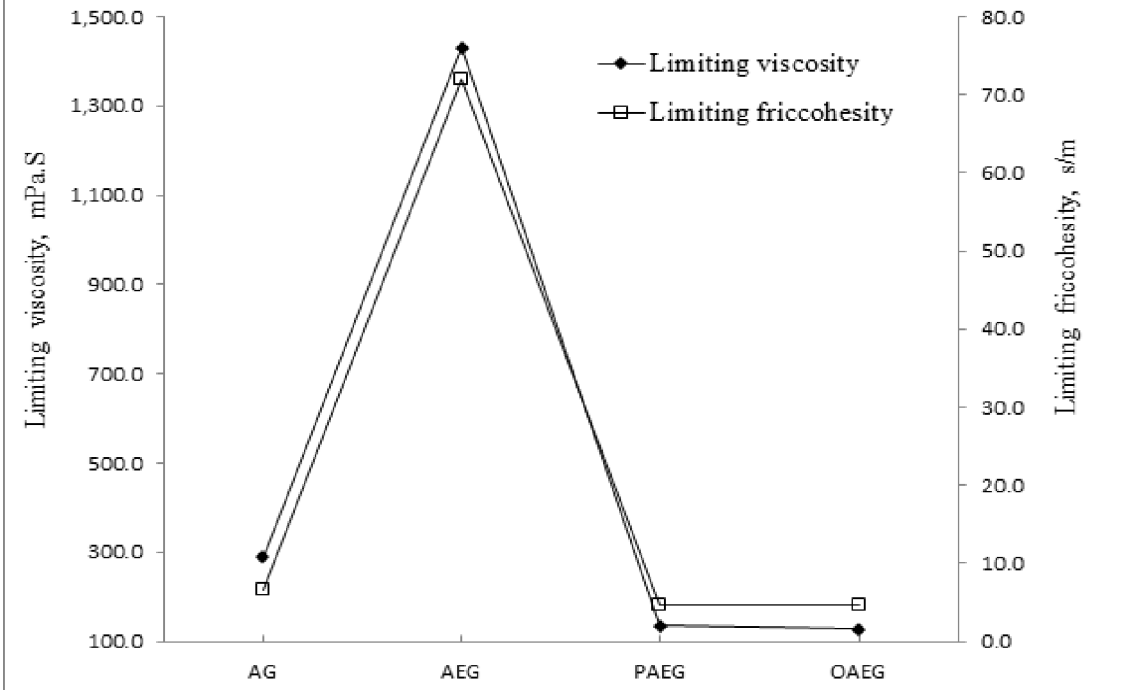

Fig. 4. Limiting density and limiting surface tension.
Fig. 5. Limiting viscosity and limiting friccohesity.

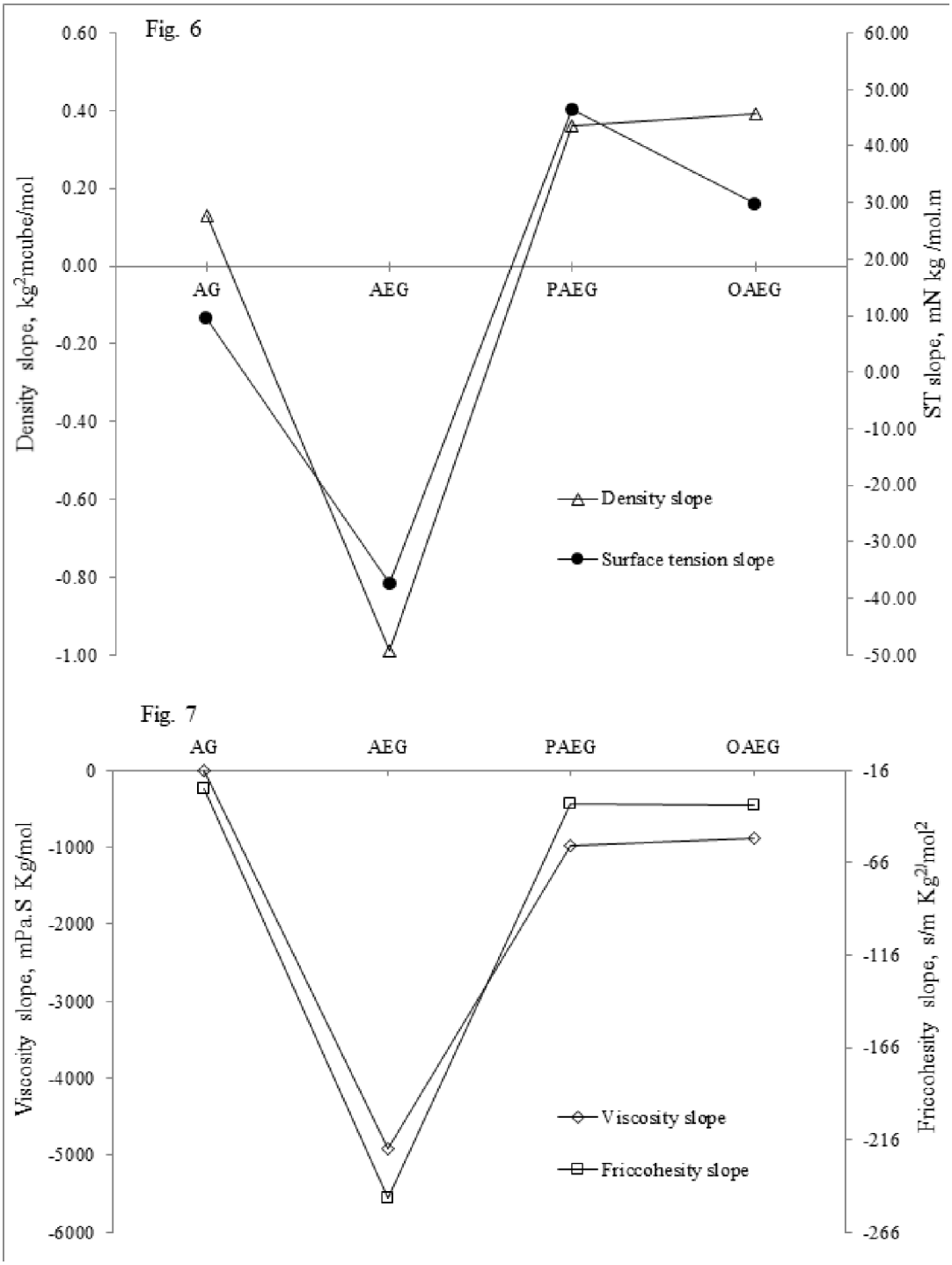

Fig. 6. Density slope and Surface tension slope.
Fig. 7. Viscosity slope and friccohesity slope.

98.87, OAE by 99.60 and PAE by 99.73%(Table 1). With Anl series a lowering of IMF is an interesting thermodynamic process and the same was achieved by solubilizing the Grl with OA and PA due to an electronic shift. For example, the USP of Anl easily donated its USEP to benzene sextet that caused interacting activities in Grl but the OA and PA with an additional -NH_2 are unable to donate their USEP whose moderation is monitored by-NH_2 of the Anl. It does not directly allow solubility with Grl and the Et has facilitated development of HB with OA, PA and Grl. It might have a 2 fold structure of Et-Grl around OA or PA benzene ring (Figs.1e, 1f). With above-mentioned electronic states the molecular combinations via HB developed thermodynamically interesting states with different PCI values given table 1 and plotted in Figs. 1d, 1e and 1f. The Grl-Grl interactions are weakened by Et, Anl, OA and PA respectively. The OAE has substantially weakened the Grl-Grl interaction and the Anl has slightly weakened as Grl-GrlI >AEGI> AGI > PAEGI > OAEGI. The -NH_2 in Anl π-conjugation is unable to develop stronger IMF as GG >AEG > AG > PAEG > OAEG. The OA and PA with -NH_2 and USEP caused stronger interactions with Grl through Et. The -NH_2 is controlling constituent of Anl derivatives for structural interactions with Grl in combination of the Et. The studies focused on stronger HB with Grl act as nonionic surfactant whereas the Anl, OA and PA as weak bases in electrophilic environment but there is no taker of their lone pair of electron (LPE). However, the LPE are shifted to benzene ring due to charge on -NH_2. The N of -NH_2 of Anl has positive charge with resonating benzene structures when the unshared electron pair is donated to adjacent N-C (Fig. 1g). The -NH_2 consists N bonded either to C or H via sigma (σ) bonds where both the C-N and -N-H bonds are polar due to electronegativity of N. These changes are fitted with equations 1 and 2 whereas trigonal pyramidal arrangement of bonds around N results into a resonance delocalisation of a lone pair into aromatic π system. A mechanism of interaction could analyze a possible contribution of electrophile behavior of Anl and nucleophile of the Grl. The medium does not support a distribution of chemical bonding except a distribution and HB formation. Though, a real potential of electrophile and nucleophile are not noted but the initiations either to favor or oppose the HB mechanism is remarkably noted in this study. There is a misconception about the HB development between O and H but a similar mechanism is established HB between Grl and Anl (Figs.1a, 1c). A polar -NH_2 has different electronegativity in H and N that resulted into HB formation.

4.4. Future prospects :

The stronger HB with Grl with 3-OH were disrupted with AG, OAEG and PAEG due to Columbic attractions that caused the intermolecular interaction that analyzed a role of medium/solvent. The factors of molecular interaction forces, dynamics and engineering contribute to structural modeling including acoustic reorientation routes to design and develop green chemistry solvents and safe reactions routes. For HVL our data could be useful for industrial and research applications where the interlocutor models could be infer interacting processes as in HVL many compounds are insoluble. If used interlocutor models can reduce the viscousness of the Grl for solublization.

5. Conclusion

Interlocutor mechanism (IM) is a smart physicochemical process to solubilize immiscible molecules without melting them by saving lot of expenditure in heat generation and other accessories for protection and safety measures. Therefore, IM is a most green and sustainable analytical device for useful mixtures out of insoluble compounds of required PCI with interacting chemical potentials. The molecules such as Et could be a most viable approach for better quality of processes of soaps, foods, pharmaceuticals, inks, dye, biotechnological, colloids, emulations, bioengineering and biochemical. A disruption of Grl HB structure with Anl series could be used in biomedical, biophysical, biochemical engineering, macromolecular chemistry and nanotechnology. Limiting density, viscosity, surface tension and

friccohesity explained the binding, surface, bulk phase, optical and acoustic activities respectively. Molecular intricacies of the OA and PA with HVL could be resolved. Unfortunately, no such work is attempted yet. The Grl with disrupted HB could be used for unfolding of proteins, biopolymers and others including lanthanide or transition metals. The Et or IM control several physicochemical properties required for mixing and solubilizing of the HVL for better applications. The Grl has 3 HB sites and aniline quickly established hydrogen bonding with higher internal pressure. Thus the parameters depend on IMF as a function of HB and polarity of Anl with concentration activities.

Acknowledgement

The Corresponding author is thankful to Prof. Shashiranjan Yadav (Honorable Vice Chancellor), Dr. Raviraj Rajpura (Registrar I/C), Dr. B. S. Patel (Dean and Principal, COE) and Dr. Tejas H. Pavagadhi (HOD, Department of Chemistry), Indian Institute of Teacher Education Gandhinagar for moral support and kind cooperation.

References

1. Yifan Yang, Qing Zheng, Yuanyuan Yan, Yao Liu, Huibo Sha., The enhanced electronic communication in ferrocene methanol molecular cluster based on intermolecular hydrogen-bonding, J. of Chinese Chem. Lett. *29*, 1, 179-182 (2018).
2. Man Singh, Sunita Singh, Inamuddin, Abdullah M. Asiri Hammadi., IFT and friccohesity study of formulation, wetting, dewetting of liquid systems using oscosurvismeter, J. Mol. Liq, 244, 7-18 (2017).
3. G. Subhapriya, S. Kalyanaraman, N. Surumbarkuzhali, S. Vijayalakshmi, V. Krishna kumar, S. Gandhimathi., Intermolecular hydrogen bonding, structural and vibrational assignments of 2, 3, 4, 5-tetrafluorobenzoic acid using density functional theory, J. Mol. Structure, *1128*, 534-543 (2017).
4. C. Y. Leo, A. Shamiri M.K. Aroua, N. Aghamohammadi R. A ramesh, Elango Natarajan, P. Ganesan, V. Akbari, Correlation and measurement of density and viscosity of aqueous mixtures of glycerol and N-methyldiethanolamine, monoethanolamine, piperazine and ionic liquid, J. Mol. Liq, *221*, 1155-1161 (2016).
5. Man. Singh, V. Kumar, R. K. Kale, C.L. Jain., Molecular activation energies ($\Delta\mu^*2$) of L-lysine, L-tyrosine, L-proline, DL-alanine, glycerol, orcinol, iodine, DTAB, and TMSOI for blending with melamine-formaldehyde-polyvinylpyrrolidone polymer resin illustrated with SEM, J. Appl. Polym. Sci., *118*, 2 960-968 (2010).
6. Man. Singh, G. V. Padmja., Synthesis, Molecular and microstructural study of poly-N-Vinylpyrrolidone Oximo-L-Valyl-Siliconate with IR, 1H-NMR and SEM, Bull., Korean Chemical Society, 31, 1874-1881 (2010).
7. Sachin B. Undre, Man Singh, R. K. Kale, Interaction behaviour of trimesoyl chloride derived 1st tier dendrimers determined with structural and physicochemical properties required for drug designing, J. of Mol Liq. *182*, 106-120 (2013).
8. Suhani Patel, Palak Patel, Sachin B. Undre, Shivani R. Pandya, Man Singh, Sonal Bakshi, DNA binding and dispersion activities of titanium dioxide nanoparticles with UV/vis spectrophotometry, fluorescence spectroscopy and physicochemical analysis at physiological temperature, J. of Mol. Liq. *213*, 304-311 (2015).
9. Man. Singh., Survismeter type I and II for surface tension, viscosity measurements of liquids for academic, and research and development studies, J. Biophys. Biochem. Methds, *67*, 151-155 (2006).
10. Man. Singh, Survismeter, 2 In 1 for viscosity and surface tension measurement, an excellent Invention for industrial proliferation of surface force in liquids, Sur. Rev. Lett. *14*, 5 973-977 (2007).
11. Man. Singh, Vinod Kumar, Solvodynamics of

benzene and water phases by DTAB, MTOAC, TMSOI and Orcinol studied with interfacial tension, surface tension and viscosity measured with Survismeter, Int. J. of Thermodynamics, *11*, 4, 181-186 (2008).

12. Man. Singh, Sushama, Studies of densities, apparent molal volume, viscosities, surface tension and free energies of activation for interactions of praseodymium Sal2en complex with dimethylsulphoxide, J. Mol. Liq.148 6-12 (2009).
13. Jarl B. Rosenholm, Critical evaluation of dipolar, acid-base and charge interactions I. Electron displacement within and between molecules, liquids and semiconductors, J. of Ad. Coll. Interf. Sci. *247*, 264-304 (2017).
14. Imteaz Ahmed, Sung Hwa Jhung, Applications of metal-organic frameworks in adsorption/ separation processes via hydrogen bonding interactions, J. of Chem. Eng., *310*, 1, 197-215 (2017).
15. Roland Böhmer Catalin Gainaru, Ranko Richert, Structure and dynamics of monohydroxy alcohols— Milestones towards their microscopic understanding, 100 years after Debye, J. of Phy. Report, 545, 4, 125-195(2014).